JACS
JOURNAL OF THE AMERICAN CHEMICAL SOCIETY
Article
pubs.acs.org/JACS

Establishing Dual Electrogenerated Chemiluminescence and Multicolor Electrochromism in Functional Ionic Transition-Metal Complexes

Egle Puodziukynaite, Justin L. Oberst, Aubrey L. Dyer, and John R. Reynolds*

The George and Josephine Butler Polymer Laboratories, Department of Chemistry, Center for Macromolecular Science and Engineering, University of Florida, Box 117200, Gainesville, Florida 32611, United States

Supporting Information

ABSTRACT: A combination of electrochromism and electroluminescence in functional materials could lead to single-layer dual electrochromic/electroluminescent (EC/EL) display devices, capable of simultaneous operation in emissive and reflective modes. Whereas such next generation displays could provide optimal visibility in any ambient lighting situation, materials available that exhibit such characteristics in the active layer are limited due to the required intrinsic multifunctionality (i.e., redox activity, electroluminescence, electrochromism, and ion conductivity) and to date can only be achieved via the rational design of ionic transition-metal complexes. Reported herein is the synthesis and characterization of a new family of acrylate-containing ruthenium (tris)bipyridine-based coordination complexes with multifunctional characteristics. Potential use of the presented compounds in EC/EL devices is established, as they are applied as cross-linked electrochromic films and electrochemiluminescent layers in light-emitting electrochemical cell devices. Electrochromic switching of the polymeric networks between yellow, orange, green, brown and transmissive states is demonstrated, and electrochemiluminescent devices based on the complexes synthesized show red-orange to deep red emission with λ_{max} ranging from 680 to 722 nm and luminance up to 135 cd/m^2. Additionally, a dual EC/EL device prototype is presented where light emission and multicolor electrochromism occur from the same pixel comprised of a single active layer, demonstrating a true combination of these properties in ionic transition-metal complexes.

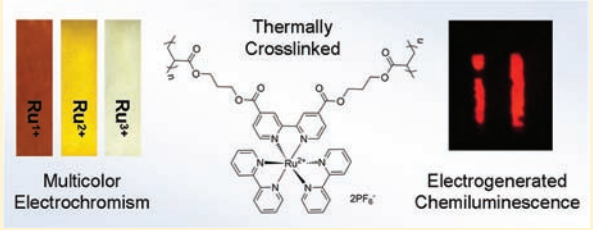

1. INTRODUCTION

Display devices based on organic electroactive small molecules and polymers have become an emerging technology due to their high contrast, low power consumption, low weight, and wide viewing angle. Additionally, there exists the possibility for display devices that exhibit mechanical flexibility, inherent processability, and optoelectronic property fine tuning via rational structure modifications of active layer materials.[1−3] While organic light-emitting diode (OLED) displays[2,4−6] have been successfully commercialized, electrochromic display devices (ECDs)[3,7−9] are finding applications in the areas of e-paper, smart windows, and large effective area information panels. Although scientific efforts remain strong in both fields, such technologies possess some intrinsic limitations. Namely, ECDs rely on external light sources and can generally be viewed only when there is sufficient ambient light available. To overcome this problem, a front or back light is provided for operation of such displays in dark conditions; however, this often results in deteriorated image quality and increased power consumption.[10] Conversely, OLEDs generally display limited visibility in bright ambient lighting situations, i.e., as the intensity of the sunlight or an ambient light source becomes stronger than that of the light emitted by the device, the displayed image bleaches.

As a result, initial attempts are being made in development of dual electrochromic/electroluminescent (EC/EL) display devices capable of simultaneous operation in reflective and emissive modes. Such systems would be emissive in low-light environments and change their colored states when sufficient light is available for a reflective mode, allowing for optimal visibility in any ambient lighting situation. Some dual EC/EL prototypes reported to date have generally been comprised of stacked ECD and OLED or light-emitting electrochemical cell (LEC) devices[11−13] as well as several layers of different active materials.[14−17] However, as a result of their complex design, poor performance and low efficiencies have been demonstrated by such systems. Recently, dual EC/EL display devices with single active layer architectures have been developed in our group.[10,18] Although the innovative construction of the devices, merging together the operating principles of ECD and LEC technologies, could offer significant advantages over the existing systems, these EC/EL display devices require active layer materials that demonstrate electrochromic and electrochemiluminescent (ECL) behavior, possess accessible oxidized and reduced states, and preferably contain motifs having ionic conductivity. While a well-balanced set of requirements for the

Received: July 13, 2011
Published: December 29, 2011

   dx.doi.org/10.1021/ja2065297 | J. Am. Chem.Soc. 2012, 134, 968−978

Scheme 1. Synthetic Route to Compound 5a

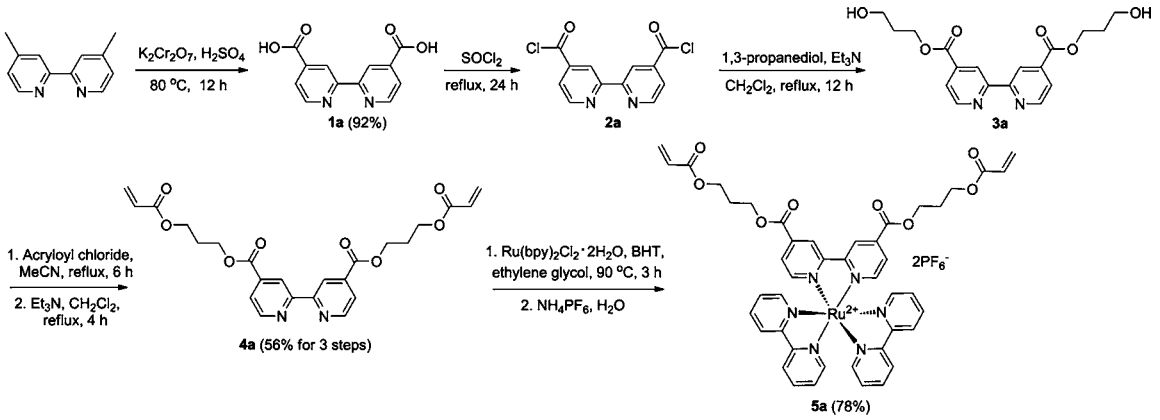

active materials is difficult to access in purely organic compounds, some ionic transition-metal coordination complexes (iTMCs) could demonstrate the required properties. Ruthenium(II) tris(bipyridine) ($Ru(bpy)_3$)-based complexes are of particular significance due to their ability to reversibly oxidize and reduce, exhibit light emission from both singlet and triplet states, display electrochromism, and possess inherent ionic conductivity.[12,19−36] In addition, photophysical and electrochemical properties of such materials can be significantly altered via rational design of the bipyridine ligands. A cumulative effect of the σ-donating and π-withdrawing ligand substituents has been previously employed to control the energies of various photoexcited states of such complexes (i.e., triplet metal-to-ligand charge-transfer excited state (^{3}MLCT), triplet metal-centered excited state, etc.) thus altering their internal conversion barriers, photoluminescence quantum yields, and emission maxima.[26,37,38] In parallel, Elliot et al. have reported that when electron-withdrawing substituents are attached at the 5,5′-positions of 2,2′-bipyridine ligands, distinct polyelectrochromic transitions can be observed for the resulting ruthenium polypyridyl complexes.[28,30,31]

While solid-state electrogenerated chemiluminescence and electrochromic behaviors have been studied separately for iTMCs, to the best of our knowledge, there have been scarce research efforts in combining these properties. Wang et al.[39] have reported on a series of polymers containing dinuclear Ru(II) complexes as pendants that exhibit electrochromism and electrogenerated chemiluminescence in the near-infrared region; however, the spectroelectrochemical properties of the compounds were only examined in solution-based optically transparent thin layer cells, and no possibility of obtaining electrochromic films insoluble in liquid electrolytes was discussed. In addition, the emission was of low efficiency. There exist a few literature precedents for organic polymers and oligomers having dual electrochromism and photo- or electroluminescence with examples being of those that contain 2-methoxy-5-(2′-ethylhexyloxy)-*p*-phenylene vinylene (MEH-PPV),[13,40,41] carbazolyl,[42] (thienylene)-[1,6-dithienylhexa-1,3,5-trienylene],[43] or fluorene-carbazole-2,5-bis(2-thienyl)-1H-pyrrole[44] repeat units as well as those that possess donor−acceptor-type architectures.[45] However, while electroluminescence (where mobile charge carriers are injected directly into π and π^* bands and move as a result of the applied field and where no doping occurs) was demonstrated in most of the reported cases, there was no evidence of electrogenerated electroluminescence in the presence of mobile ions (the operating principle of an LEC);[11] a necessity for a single material that is to be employed as both a light emitter and an electrochrome in the same device. Moreover, such highly nonpolar structures are known to often exhibit strong phase separation when blended with polar, ion transporting materials, such as polyethylene oxide, which is essential to achieve adequate ionic conductivity in the corresponding electrochemical devices. Such phase separation results in strong aggregation and electroluminescence quenching of the light-emitting polymers as well as inferior lifetimes of the respective devices.[46] Meanwhile, as MEH-PPV has been extensively applied in light-emitting electrochemical cells, it suffers from poor redox reversibility and, as a result, poor electrochromic properties, including the lack of the ability to access a highly transmissive, near colorless state needed for practical applications.

As functional Ru(II) complexes previously reported in the literature for electrochromism and electrochemiluminescence generally differ in structure and are optimized only for a single application, the purpose of this study is to understand the relationship between the detailed ligand design and combined EC/EL behavior of the resulting compounds. Thus, reported herein is a new family of ruthenium(II) tris(bipyridine) coordination complexes, combining intrinsic electrochromism, electrochemiluminescence, ionic conductivity, and reversible redox behavior. To study the structure−property relationships as well as to induce color tuning of the emissive and reflective states of the complexes, the iTMCs are functionalized with both electron-withdrawing and -donating substituents at various positions. Two reactive acrylate moieties are introduced into the structures allowing for insoluble film formation upon thermal cross-linking and for the films to be utilized in the presence of liquid electrolytes or gel electrolytes without risk of dissolution upon application in dual EC/EL devices. This diacrylate approach is shown to be synthetically robust giving materials with a long shelf life when compared to the previously reported hexaacrylate derivatives.[26,31] Electrochemical, spectroscopic, and full colorimetric characterizations are given for the compounds synthesized. Dual character of the reported complexes is established, as they are applied as cross-linked electrochromic films and electrochemiluminescent layers in LEC devices. Switching of the corresponding polymeric networks between yellow, orange, orange-red, green, brown and transmissive states is demonstrated, and orange-red to deep red emission with λ_{max} ranging from 680 to 722 nm is obtained from LEC devices, comprised of the compounds reported as

dx.doi.org/10.1021/ja2065297 | J. Am. Chem.Soc. 2012, 134, 968−978

Scheme 2. Synthetic Route to Compound 5b

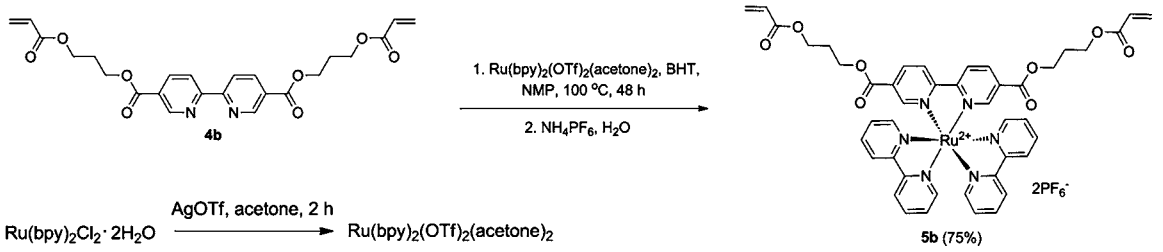

their active materials. It is shown that the complexes synthesized retain their ECL character upon cross-linking, enabling their application in electrochemical devices containing liquid electrolyte, while simultaneously leading to advanced architectures of the resulting active layers. Moreover, the EC and ECL properties of the iTMCs are demonstrated to be truly paired, as they are applied in a dual EC/EL device prototype, where light emission and multicolor electrochromism occurs from a single Ru(II)-based active layer within a single pixel.

2. RESULTS AND DISCUSSION

2.1. Synthesis. $Ru(bpy)_3$-based diesters **5a** and **5b** were synthesized via similar multistep routes, as depicted in Schemes 1 and S1 in the Supporting Information. Compounds **1a** and **1b** were obtained by the oxidation reactions of 4,4′-dimethyl-2,2′-bipyridine and 5,5′-dimethyl-2,2′-bipyridine, correspondingly, with potassium dichromate in sulfuric acid. Compounds **4a** and **4b** were then synthesized by employing a minimal-purification multistep route modified from that previously described in the literature.[26,31] Briefly, diacids **1a** and **2a** were refluxed in thionyl chloride for 24 h to give diacid chlorides **2a** and **2b**, which were immediately converted to their ester derivatives by employing an addition−elimination reaction with 1,3-propanediol in the presence of triethylamine. The resulting products **3a** and **3b** were then reacted with acryloyl chloride to give compounds **4a** and **4b** in 56% and 52% overall yields, correspondingly. Compound **5a** was then synthesized by employing well-established complexation with $Ru(bpy)_2Cl_2{\cdot}2H_2O$ and ion metathesis procedures (Scheme 1). Complex **5b** (Scheme 2), however, could not be obtained using the same protocol as for **5a** due to the transesterification reactions of the ester moieties at 5,5′-positions with the alcoholic solvents, i.e., ethylene glycol, methanol, and ethanol. A similar observation has been recently reported by Grabulosa et al.[47,48] In addition, further evidence, although not very detailed, for such side reactions can be found in the literature.[48] The observed transesterification reactions could be partially inhibited by using sterically hindered secondary alcohols as solvents; however, a large decrease in the rate of the complexation reaction was also observed. Thus, the desired product **5b** could only be efficiently synthesized by the complexation reaction of **4b** and the activated ruthenium complex $Ru(bpy)_2(acetone)_2(OTf)_2$[49,50] in *N*-methylpyrrolidone (Scheme 2). It is noteworthy, that the use of butylated hydroxytoluene as a free radical scavenger resulted in significantly increased yields of the complexation reactions via inhibition of acrylate polymerizations.

Compounds **9a** and **9b**, having alkyl-substituents at the 4,4′- and 5,5′-positions, respectively, were synthesized according to Scheme 3. Starting materials **6a** and **6b** (for the synthesis of **8b**, see Scheme S2 in Supporting Information) were obtained by esterification reactions from the corresponding diacids and

Scheme 3. Synthetic Route to Compounds 9a and 9b

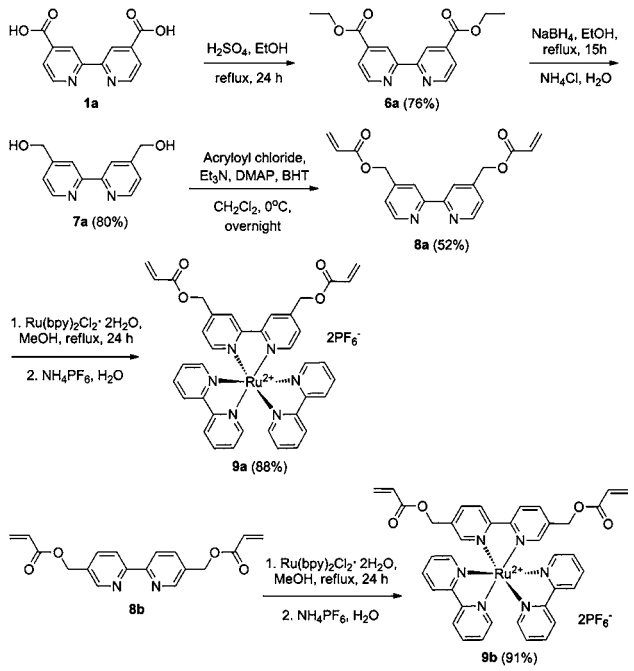

ethanol in the presence of sulfuric acid as a catalyst. The esters synthesized were later converted to dialcohols **7a** and **7b** using sodium borohydride, reacted with acryloyl chloride, and used in the complexation reactions with $Ru(bpy)_2Cl_2{\cdot}2H_2O$ to give target molecules **9a** and **9b**.

2.2. Electrochemistry. The electrochemical properties of complexes **5a, 5b, 9a** and **9b** were studied in 0.1 M tetrabutylammonium hexafluorophosphate ($TBAPF_6$) acetonitrile solutions using platinum button, platinum flag, and silver wire (calibrated versus the ferrocene/ferrocenium standard redox couple) as working, counter, and reference electrodes, respectively. The cyclic voltammograms and the corresponding half-wave redox potentials for compounds **5a**, **5b**, and **9a** are given in Figure 1. The cyclic voltammogram of **9b**, essentially analogous to that of **9a**, is provided in Figure S1 in Supporting Information.

It has been well-established that the electrochemical behavior of Ru(II) polypyridyl complexes is usually observed as a metal-centered oxidation and a series of ligand-centered reductions.[19] As a result, reversible oxidations were characteristic of all the ruthenium(II) complexes reported with the corresponding $E_{1/2}$ values only somewhat cathodically shifted for compounds **9a** and **9b** with respect to those of their diester analogues **5a** and **5b** due to the electron-donating character of the alkylester substituents on the bipyridine ligands. Conversely, significantly pronounced substituent effects upon reduction of the studied complexes were evident. Complexes **5a** and **5b**, having

dx.doi.org/10.1021/ja2065297 | J. Am. Chem.Soc. 2012, 134, 968−978

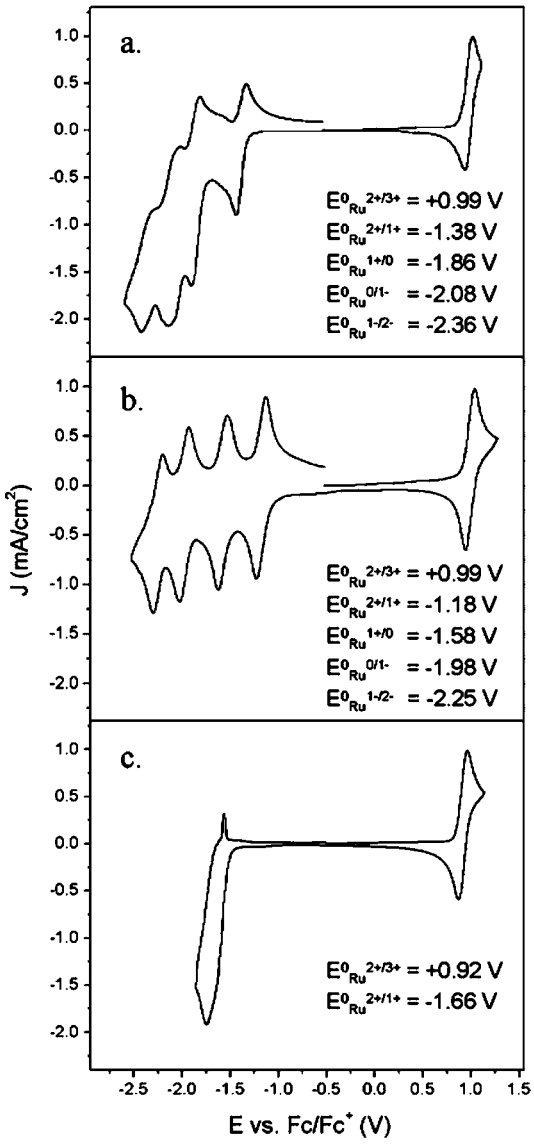

Figure 1. Cyclic voltammograms of compounds **5a** (a), **5b** (b), and **9a** (c) in 0.1 M $TBAPF_6$ acetonitrile solutions at 100 mV/s scan rate. Platinum button, platinum flag, and silver wire (calibrated versus the ferrocene/ferrocenium standard redox couple) were used as working, counter, and reference electrodes, correspondingly.

electron-withdrawing ester moieties, were verified to possess four reduction waves that were anodic with respect to those of **9a** and **9b**. Stabilization of anion radicals was particularly evident in the case **5b**, as seen from the well-defined reduction peaks with excellent reversibility, indicating a significant extent of lowest unoccupied molecular orbital (LUMO) present on the carboxyl functionalities of the bipyridine ligand.[30] Moreover, although a 'localized model' is generally used to explain reduction processes in ruthenium polypyridyl complexes (i.e., each additional electron is stabilized on a specific ligand),[19] for **5b**, even remote reduction waves occurred at potentials ca. 100 mV more positive than those for **5a**, demonstrating some delocalized character. Compounds **9a** and **9b** possessed one reversible reduction band, whereas other similar transitions were significantly destabilized. In addition, with such dialkylester-substituted bipyridine ligands being more difficult to reduce, preferential electrochemical polymerization of the acrylate moieties was observed for the complexes upon cycling (see Figure S2 in Supporting Information).[51]

2.3. Spectroelectrochemistry. In order to study the spectroelectrochemical properties of the compounds synthesized, ruthenium complexes **5a** and **5b** were mixed with trimethylolpropane triacrylate (TMPTA) and tetraethyleneglycol dimethacrylate (TEGDMA) as auxiliary cross-linking agents and cast on ITO/glass transparent electrodes by spin coating followed by thermal cross-linking to yield insoluble polymer films. To demonstrate the ability to introduce additional colored states and the possibility for designed color tuning, the copolymer of **5a** and **5b** in 1:1 molar ratio (**5a**-*co*-**5b**) was also prepared. To overcome poor electrode wetting effects and attain uniform coatings with glassy morphology, 5 wt % of poly(methyl methacrylate) (PMMA) was used in the case of **9a** and **9b** in addition to the auxiliary cross-linking agents. All insoluble films obtained demonstrated electroactive character with polyelectrochromic transitions as determined by spectroelectrochemical and colorimetric studies. Spectroelectrochemistry data for the polymeric films of complexes **5a**, **5b**, their copolymer in 1:1 molar ratio (**5a**-*co*-**5b**), **9a**, and **9b** at all the stable formal redox states were assessed and are given in Figure 2 (spectroelectrochemistry data for **9b** is provided in Figure S3 in Supporting Information). For each of the complexes, including the blend film, the as-cast 2+ oxidation state exhibited an absorption centered around 450 nm with each differing in the intensity and breadth of that absorption, resulting in various hues of yellow, orange, or tan for each complex. Once oxidized to the 3+ oxidation state, all the studied polymer films demonstrated bleaching of MLCT bands and a subsequent change from colored to transmissive states. However, upon reduction of the 2+ state, spectral trend differences for each of the complexes became significantly pronounced. Poly-**5a** demonstrated only a small increase in absorption intensity as well as a 10 nm red shift for λ_{max} at the 1+ oxidation state, resulting in a dark red-orange color. Poly-**5b** exhibited an additional absorption band with the maximum at λ_{abs} = 675 nm in addition to substantially pronounced absorption increase at each reduced state, resulting in corresponding dark blue-green and subsequent dark orange colors for the 1+ and 0 oxidation states, respectively. Two rational explanations of such a distinct polyelectrochromic effect demonstrated by poly-**5b** could be attributed to electronic transitions between closely spaced molecular orbitals with near degeneracy as well as intraligand charge-transfer processes.[30] The cumulative spectroelectrochemical behavior of the complexes **5a** and **5b** was characteristic of their copolymer (Figure 2c), resulting in switching between intermediate colored states. It is noteworthy that while additional reduced states could be accessed for most of the studied compounds, as is shown in the cyclic voltammograms of Figure 1, the reversibility of such redox transitions was limited by either stability of the solvent window, formation of mixed valence states upon cycling, or dissolution of the polymeric films. For instance, the 1+ oxidation state for poly-**9a** did not prove to be spectroelectrochemically beneficial, as the cross-linked film dissolved upon repeated switching between the 2+ and the 1+ redox states.

2.4. Colorimetry. Colorimetry studies were carried out on the electrochromic polymer networks obtained, allowing for effective quantification of their color as it is perceived by the human eye. The 1976 CIE LAB (or $L^*a^*b^*$) color space has been chosen as a standard method of color representation,

dx.doi.org/10.1021/ja2065297 | J. Am. Chem.Soc. 2012, 134, 968–978

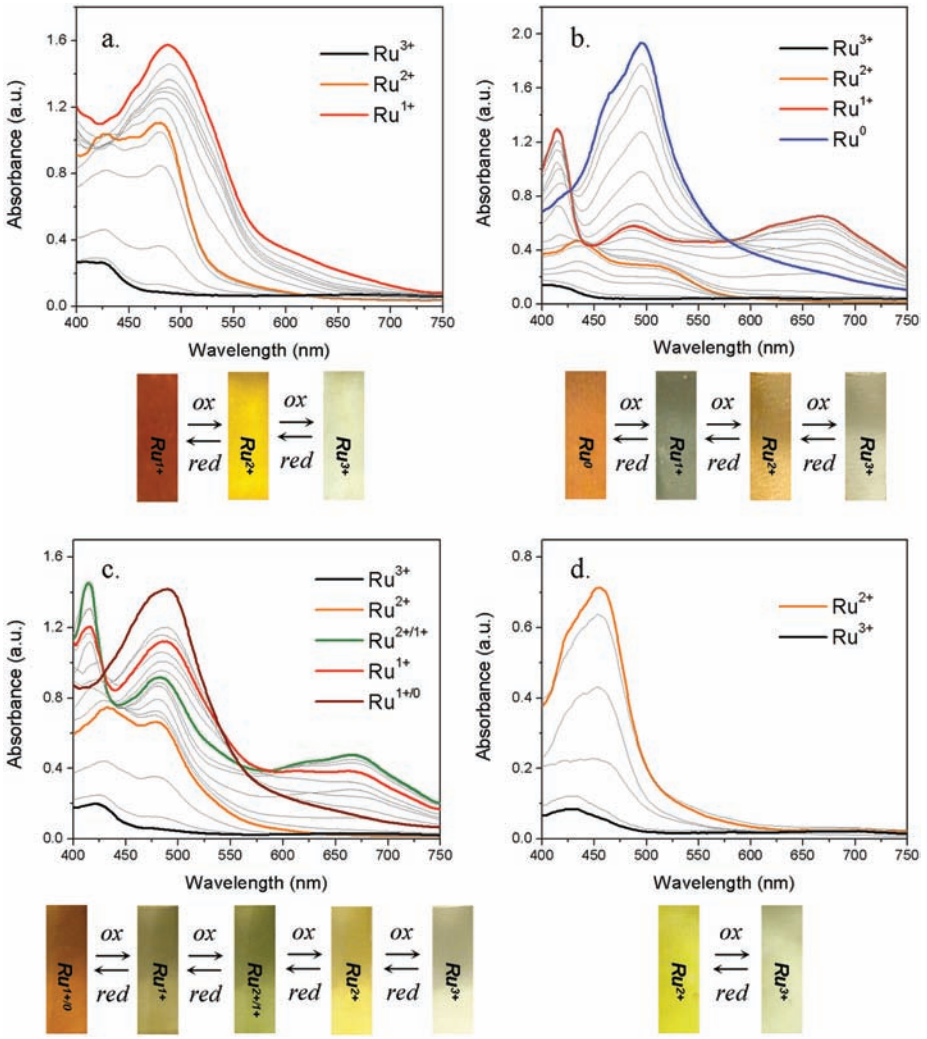

Figure 2. Spectroelectrochemistry data and the corresponding photographs of the polymeric films of **5a** (a), **5b** (b), **5a** and **5b** blend in 1:1 molar ratio (c), and **9a** (d) at all the unambiguously stable redox states in 0.1 M $TBAPF_6$ acetonitrile solutions. ITO/glass, platinum flag, and silver wire (calibrated versus the ferrocene/ferrocenium standard redox couple) were used as working, counter, and reference electrodes, correspondingly.

where the L^* value corresponds to the lightness of the material, a^* indicates red-green balance, and b^* designates yellow-blue balance of the substance. Additionally, the terms of hue, saturation, and luminosity are used in color specification. Hue is generally described by the dominant absorption wavelength, saturation refers to the dominance of hue in the color and increases toward the edges of the a^*b^* color wheel, while luminosity represents the amount of white in the color and is related to L^*. In this study, $L^*a^*b^*$ chromaticity coordinates were calculated from the absorbance spectra of the polymer films at all their studied redox states using methods standardized by CIE.[52,53] In an effort to verify the accuracy of the chosen technique, color coordinates of the polymer networks at their as prepared 2+ redox states were also measured using a Minolta CS-100 colorimeter (transmission measurement method)[54] and were found to be in good agreement with those calculated. $L^*a^*b^*$ chromaticity coordinates for compounds **5a**, **5b**, **5a-co-5b**, **9a**, and **9b** at all their studied redox states are summarized in Tables 1 and 2.

In the as prepared 2+ oxidation state, compounds **5a**, **5b**, and **5a-co-5b** were verified to have orange color exemplified by the large positive a^* and b^* values, while compounds **9a** and **9b** possessed hues in the pure yellow region exemplified by the relatively small a^* and large b^* values. Such a finding was in good agreement with the spectral data (Figure 2), where all the compounds in their 2+ oxidation state absorbed wavelengths attributed to either blue or green light. As detailed earlier, the reduced states of the polymeric films exhibited complex spectral profiles with multiple absorption peaks and variances in intensity making the exact color displayed by the film difficult to determine by absorbance spectra alone. The use of colorimetry in this situation could provide valuable insight

Table 1. CIE 1976 $L^*a^*b^*$ Values[a] for the Thermally Crosslinked Films of Compounds 5a, 5b, 9a, and 9b at Various Redox States

compound/ redox state	5a	5b	9a	9b
3+	94, −1, 9	96, −1, 2	98, −1, 5	97, 0, 7
2+	86, 12, 85 (89, 13, 83)	88, 14, 32 (92, 13, 35)	96, −3, 46 (95, 3, 55)	94, −1, 51 (96, 3, 57)
1+	66, 31, 66	63, −8, 2	–	–
0	–	63, 29, 58	–	–

[a]Values were calculated from the absorbance spectra of the cross-linked films. Given in brackets are CIE 1976 $L^*a^*b^*$ values measured with a Minolta CS-100 colorimeter.

dx.doi.org/10.1021/ja2065297 | J. Am. Chem.Soc. 2012, 134, 968−978

Table 2. CIE 1976 $L^*a^*b^*$ Values[a] for the Copolymeric Film of 5a and 5b in 1:1 Molar Ratio at Various Redox States of 5a and 5b

	5a	3+	2+	2+	1+	1+
redox state	5b	3+	2+	1+	1+	0
$L^*a^*b^*$		98, −1, 9	87, 13, 56 (91, 13, 62)	66, 3, 36	66,14, 45	73, 27, 70

[a]Values were calculated from the absorbance spectra of the cross-linked films. Given in brackets are CIE 1976 $L^*a^*b^*$ values measured with a Minolta CS-100 colorimeter.

into the colors observed, verifying those shown in the photographs in Figure 2. Specifically, the reduced poly-**5a** film (1+ oxidation state) had a decrease in L^*, an increase in a^*, and a decrease in b^* values indicating a darker orange-red color relative to the 2+ oxidation state. For the two reduced states of poly-**5b** (1+ and 0 oxidation states), the L^* value remained the same, while significant changes were observed in the a^* and b^* values with the film changing from a blue-green to an orange-red color. The colorimetric values for the copolymer of **5a** and **5b** also showed the subtleties in the differences between the colors exhibited by each of the mixed valence states with additional switching to dark green-brown and gray-brown states (Table 2) due to color mixing. A slight mismatch between the green color observed in the photographs and the calculated $L^*a^*b^*$ values for this copolymer film in the 2+/1+ mixed oxidation state could possibly be due to subtleties in color perception associated with a low a^* value of 3. Conversely, as a result of loss of their MLCT absorption bands, all the studied compounds were switched to nearly colorless, highly transmissive states upon oxidative bleaching, as designated by significantly lower a^* and b^* values as well as L^* values as high as 98 (Table 1).

While these Ru(II) complexes reported herein are attractive candidates for multicolored ECD-type device applications, we have previously emphasized that electrochromic window and display devices require solution processable active layer materials that are capable of switching from a vibrantly colored state to a colorless, transmissive state.[55] As such, the orange and yellow Ru(II)-based electrochromes **5a** and **9a** were chosen to be further characterized in terms of electrochromic contrast (percent transmission change, $\Delta\%T$) and color difference (ΔE) when switched between the colored and bleached states.[56] The orange and yellow electrochromes were chosen as yellow is one of the primary subtractive colors that are used to access any color of the visible spectrum in reflective displays (R−Y−B and C−M−Y). Moreover, such transitions are generally difficult to achieve in organic polymeric electrochromes, and the corresponding prototypes have only recently been reported by our group in completion of the color palette of electrochromic spray-processable polymers (ECPs).[57−59] While $\Delta\%T$ is defined as the difference in percent transmittance between the clear and the dark states of the material at one particular absorption wavelength, color difference [i.e., $\Delta E = \{(\Delta L^*)^2 + (\Delta a^*)^2 + (\Delta b^*)^2\}^{1/2}$] takes into account differences in all three color coordinates of an electrochrome at two colored states and mathematically can be described as a vector connecting the two states in the three-dimensional $L^*a^*b^*$ color space. The obtained optical data for compound **5a** and **9a** cross-linked films, in addition to the recently reported polymer electrochromes poly(3,4-di(2-ethylhexyloxy)-thiophene) (ECP-orange) and a substituted poly-(propylenedioxythiophene-*alt*-phenylene) (ECP-yellow) are summarized in Table 3. Additionally, CIE 1976 a^*b^* values

Table 3. Percent Transmission Contrast ($\Delta\%T$) and Color Difference (ΔE) Data for 5a, 9a, ECP-Orange, and ECP-Yellow, as They Switch from Vibrantly Colored to Transmissive States[a]

compound	color	$\Delta\%T$ (λ_{max})	ΔE
5a[b]	orange	74% (480 nm)	78
5a[c]	orange	80% (487 nm)	72
9a	yellow	68% (456 nm)	50
ECP-O	orange	48% (485 nm)	75
ECP-Y	yellow	73% (456 nm)	64

[a]Values for ECP-O and ECP-Y are are of similar optical density for λ_{max} of the colored state to those indicated for the iTMC polymer films. [b]Redox transition (2+ → 3+). [c]Redox transition (1+ → 3+). $\Delta\%T$ values are calculated at the wavelengths indicated.

for poly-**5a** and poly-**9a** at their stable and reversible redox states are plotted in Figure 3 to illustrate their orange and

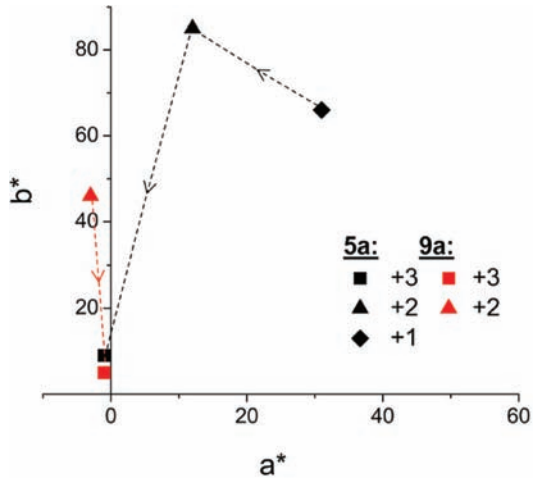

Figure 3. CIE 1976 a^*b^* values for cross-linked films of **5a** and **9a** calculated from their absorption spectra at all the unambiguously reversible redox states.

yellow to transmissive transitions. Here, the b^* value changes for **9a** from 46 to 5 demonstrating the yellow to nearly colorless switch, while the orange hues evident for **5a** in the 2+ and 1+ oxidation states convert to the transmissive state with the a^*b^* values of −1 and 9, respectively, upon oxidation. As is evident by examining the optical data, Ru-iTMCs studied have high transmission contrast and color difference values, which are comparable to state-of-the-art orange and yellow to transmissive ECP electrochromes.

2.5. Emission Spectra. Normalized photoluminescence spectra from thin solid films of complexes **5a**, **9a** and **9b** are given in Figure 4. It has been well-established that, due to spin−orbit coupling and efficient intersystem crossing, light

dx.doi.org/10.1021/ja2065297 | J. Am. Chem.Soc. 2012, 134, 968−978

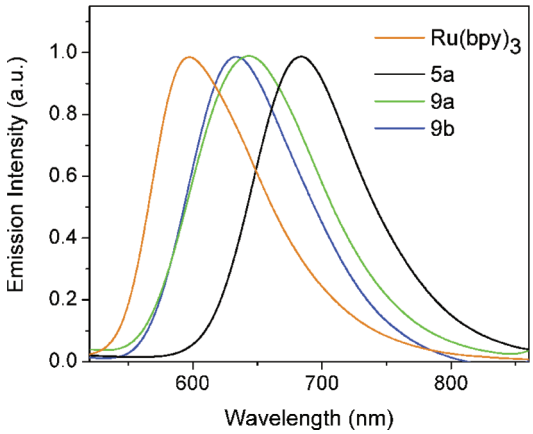

Figure 4. Photoluminescence spectra of compounds **5a**, **9a**, **9b**, and $Ru(bpy)_3 \cdot 2PF_6$ in solid state (normalized) at excitation wavelength λ_{exc} = 450 nm.

emission from Ru-iTMCs mostly occurs as phosphorescence with broad unstructured emission bands characteristic of MLCT electronic transitions.[19,60,61] Accordingly, the studied compounds demonstrated broad featureless photoluminescence profiles in the orange-red and red regions with the emission maxima at 640 nm for the complexes **9a** and **9b** and 680 nm for their diester analogue **5a**. The red shift of ca. 40 nm in the emission of compound **5a** was hypothesized to arise from a decrease in its ligand-based LUMO value and the resulting lower energy MLCT transitions. No significant spectral differences were observed for the photoluminescence properties when compounds **5a**, **9a**, and **9b** were compared in degassed acetonitrile solutions (see Figure S5 in Supporting Information) and solid state. Conversely, complex **5b**, having ester substituents at 5,5′-positions showed weak photoluminescence with λ_{max} = 700 nm in solution, whereas no light emission was detected in the solid state. Such spectral behavior of this complex is consistent with literature examples[62] and can be partially attributed to the energy gap law for such complexes.[38,63−65] Photoluminescence quantum yield values for complexes **5a**, **9a**, and **9b** in deaerated acetonitrile solutions were assessed using $Ru(bpy)_3 \cdot 2PF_6$ as a standard and were found to be Φ_E = 8.1, 13.1, and 10.3%, respectively.

2.6. Light-Emitting Electrochemical Cells. In an effort to explore the electrochemiluminescent behavior of the compounds reported, LEC devices,[13,24,25,66−71] comprised of the newly synthesized ruthenium complexes **5a**, **5b**, **9a**, and **9b** as active materials, were fabricated. The LEC devices studied were comprised of an ITO/glass anode onto which the active electroluminescent layer was prepared by spin coating from a solution of the Ru(II) polypyridyl complex and 21 wt % of PMMA in acetonitrile, followed by a thermally evaporated gold cathode. The PMMA was utilized as a supporting polymer matrix as it results in an improved film quality and higher overall device efficiencies, as has been previously reported in the literature.[72] Immediately prior to optical and electrical measurements of the devices, a precharging of each pixel was performed, wherein a short, high voltage bias was applied (typically ∼1−2 V higher than that necessary for initial light output) causing redistribution of charge-balancing ions at the anode and cathode but not resulting in degradation of active layer materials. This method has been previously demonstrated in the literature to give nearly instantaneous device response even at low voltages that otherwise cause sluggish turn-on times (on the order of minutes to hours) for pristine devices.[27]

As can be seen in the emission spectra and pixel photographs in Figure 5, all devices exhibited emission evenly across the

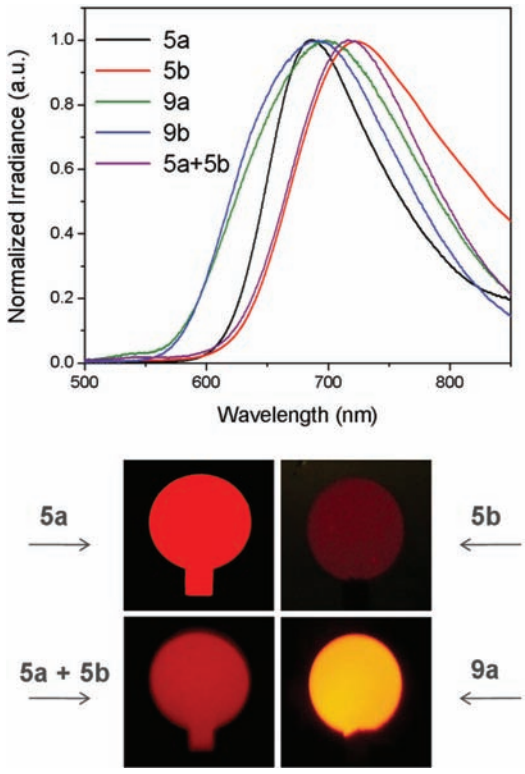

Figure 5. Normalized EL spectra of LECs based on **5a**, **9a**, and **9b** biased at 4.5 V and **9a** as well as the blend of **5a** and **5b** in 1:1 molar ratio biased at 7 V and the corresponding photographs of the LEC pixels (diameter = 3 mm).

entire pixel with the devices comprised of the Ru-based iTMCs **5a** and **5b** exhibiting emission with λ_{max} values ranging from 688 to 722 nm, coinciding with the solution and solid-state photoluminescence spectra, while those comprised of complexes **9a** and **9b** exhibited significant bathochromic shifts of ca. 50 nm from their solution and solid-state photoluminescence spectra. We hypothesize that this is due to destabilization of the excited states upon device operation resulting from electrochemically induced chemical side reactions that are occurring at the acrylate sites, hampering electron injection events resulting in the ca. 50 nm bathochromic shift in emission maxima and lower light output as will be discussed later.[73] This hypothesis is supported by extensive cyclic voltammetry studies (see Figure S2 in Supporting Information) where the reductive polymerization of the complexes occurred at approximately the same potential as their first reductions.

These differences in optical properties between the complexes were also noted in colorimetric measurements of the emitted light, presented as the CIE *x,y* color coordinates in Table 4. Devices comprised of **5a** and **5b** showed ECL response in the red region with *x,y* coordinate values x = 0.68, y = 0.32 and x = 0.67, y = 0.29, respectively. Dimethylesters **9a** and **9b**, although having ca. 10 nm bathochromically shifted ECL maxima when compared to that of **5a** devices, showed emission color coordinates (x = 0.64, y = 0.36 and x = 0.65, y = 0.34, correspondingly) that were characteristic of red-orange

dx.doi.org/10.1021/ja2065297 | J. Am. Chem.Soc. 2012, 134, 968−978

Table 4. Optical and Efficiency Characteristics As Well As Time Required to Reach Half of the Peak Radiant Exitance Value (Precharged Mode) Of the LEC Devices Based on Compounds 5a, 5b, 9a, 9b, and the Blend of 5a and 5b (1:1 Molar Ratio) at the Indicated Voltages

compound	λ_{max} (nm)	CIE (x,y) coordinates	peak radiant exitance (μW/cm^2)	peak luminance (cd/m^2)	max. EQE (%)	EQE at peak light output (%)	$\tau_{1/2}$ (s)
5a	688	(0.68, 0.32)	1031.0 (5.5 V)	153.0 (5.5 V)	2.22 (3.0 V)	0.49 (5.5 V)	2 (5.5 V)
5b	722	(0.67, 0.29)	48.9 (6.0 V)	2.0 (6.0 V)	0.04 (4.0 V)	0.03 (6.0 V)	2 (6.0 V)
9a	699	(0.64, 0.36)	220.2 (5.5 V)	56.4 (5.5 V)	0.11 (3.5 V)	0.03 (5.5 V)	2 (5.5 V)
9b	692	(0.65, 0.34)	32.1 (6.0 V)	16.7 (6.0 V)	0.37 (3.5 V)	0.02 (6.0 V)	1 (6.0 V)
5a+5b	717	(0.67, 0.34)[a]	40.0 (6.0 V)	2.0[a] (6.0 V)	0.05 (4.0 V)	0.02 (6.0 V)	1 (6.0 V)

[a]Values were calculated from spectral and radiant exitance data.

emission. This is not unexpected given that, while the peak emission occurs at longer wavelengths, the increased emission in the range from ca. 550 to 600 nm contributes substantially to the color observed, as these wavelengths are the region where the human eye is the most sensitive.

Table 4 presents the optical properties (radiant exitance and luminance) and efficiencies [external quantum efficiency (EQE)] measured for LEC devices containing each of the complexes in addition to the **5a**/**5b** blend. We report both luminance and radiant exitance data, as the luminance is the most common representation of light output for visible displays, while it is also desired to understand the total power emitted for a more fundamental understanding of device performance. The voltage dependence of both radiance exitance and luminance is shown in Figure S6 in Supporting Information. Additionally, we present both maximum external quantum efficiency (EQE_{max}), which may occur at lower voltages and minimal light output due to the low current densities and the EQE at the peak light output (peak EQE). As can be seen, LEC devices containing **5a** demonstrated the brightest light output with radiant exitance values as high as 1.03 mW/cm^2 and the EQE_{max} of 2.22%. These performance results are consistent with similar systems presented in the literature with examples of pristine LEC devices comprised of Ru(II) bis(2,2′-bipyridine)(dimethyl-[2,2′-bipyridine]-4,4′-dicarboxylate) bis(hexafluorophosphate) and Ru(II) tris-(dimethyl-[2,2′-bipyridine]-4,4′-dicarboxylate) bis(hexafluorophosphate) having red ECL response with λ_{max} = 690 nm and EQEs of 0.1−0.4% at 3−5 V.[27] It is notable that EQE_{max} values as high as 5.5% have been reported in the literature for Ru-based LECs, however, the corresponding devices were operated under very specific pulsed voltage conditions to obtain the maximum performance.[74] It is interesting to note that, although a weak solution photoluminescence response (and no solid-state photoluminescence response) was observed for compound **5b**, LECs based on the complex demonstrated visible light emission upon electroexcitation. While a significant decrease in radiant exitance, luminance, and EQE values were observed for devices comprised of **5b** as well as for devices based on the blend of **5a** and **5b** (1:1 molar ratio), this observation can be partly attributed to the strongly red-shifted low-energy light emission of the respective LECs. Additionally, it is noteworthy that devices comprised of **5b** and the blend of **5a** and **5b** (1:1 molar ratio) as their active layers are among the deepest red light-emitting mononuclear Ru(II) complex-based LECs reported in the literature with their emission wavelength and EQEs comparable to those reported by Bolink et al.[75] The performance of **9a**- and **9b**-based devices was lower than that demonstrated by similar Ru(II)-based systems[27] and, as explained above, resulted from the possible destabilization of the excited states caused by the electrochemical side reactions during device operation.[73]

As mentioned previously, for ultimate application as the active layer in a dual EC/EL device, the electroluminescent material should be that of an insoluble, electrode supported film. To demonstrate the ability of these Ru(II)-based LECs to retain their emissive properties (color and intensity) when employed as insoluble films, we studied LEC devices where the active layer is cross-linked, as was performed for the electrochromism study. As the molecular LEC devices comprised of compound **5a** demonstrated best overall performance, we further studied this system as the cross-linked electrochemiluminescent layer in the polymeric LEC devices. The active layers were cast as thin films by spin coating, onto ITO/glass anodes, from a solution containing compound **5a**, 21 wt % of TEGDMA, and 0.5 wt % of azobisisobutyronitrile (AIBN) in acetonitrile. The active layer was then subjected to thermal cross-linking by heating at 150 °C for 12 h, and a gold cathode was deposited as previously described. In such devices, TEGDMA served as both a cross-linking agent and a supporting matrix replacing PMMA. Initial devices prepared in this manner had the ultimate film thickness much lower (ca. 50%) than that of the molecular LECs, resulting in electrical shorts. As such, as second film deposition process was added to create two sequentially deposited, cross-linked bilayers to increase the film thickness. As is indicated by radiant exitance measurements shown in Figure 6 and the spectral data provided in Table 5, while the light output at lower applied voltages was less intense for the multilayer device compared to the single layer, molecular device, the peak light output in the multilayer

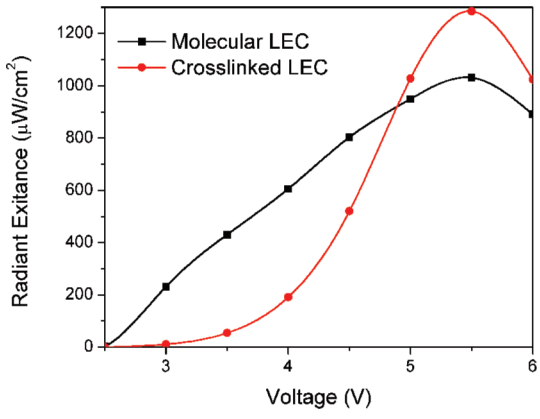

Figure 6. Voltage-dependent radiant exitance for LEC devices comprised of **5a** as a molecular compound blended with PMMA (black squares) and those comprised of **5a** as a polymer cross-linked with TEGDMA (red circles).

dx.doi.org/10.1021/ja2065297 | J. Am. Chem.Soc. 2012, 134, 968−978

Table 5. Optical and Efficiency Characteristics As Well As Time Required to Reach Half of the Peak Radiant Exitance Value (Precharged Mode) of the LEC Devices Based on 5a as a Molecular Compound Blended with PMMA and Those Comprised of 5a as a Polymer Cross-Linked with TEGDMA at 5.5 V

supporting matrix	λ_{max} (nm)	CIE (x,y) coordinates	peak radiant exitance (μW/cm^2)	EQE at peak light output (%)	$\tau_{1/2}$ (s)
PMMA	688	(0.68, 0.32)	1031.0	0.49	2
TEGDMA	682	(0.70, 0.30)	1284.9	0.27	2

cross-linked devices demonstrated slightly elevated ECL performance and an emission color comparable to that of their molecular prototypes. The decrease in the EQE values and light output at lower operating voltages after cross-linking is possibly due to inhibition of functional group local motion, leading to decreased counterion mobility and charge transfer, as expected when comparing molecular and polymeric systems. The device characterization results show, however, that the cross-linking process, necessary to produce thin films of the complexes for use in dual EC/EL devices, is not detrimental to the light-emitting properties or emission color, which is the first step in demonstrating the applicability of these systems in the dual-mode devices.

2.7. Dual EC/EL Device Prototype. In an effort to demonstrate that dual electrochromic and electrogenerated chemiluminescence response can be observed from a single active material layer in a single device architecture, dual EC/EL device prototypes have been constructed. In accordance with the fabrication of the polymeric LEC devices, complex **5a** has been chosen as the basis for the dual EC/EL prototype active film. As shown schematically in Figure S8 in Supporting Information, the device was fabricated by spin coating the active layer, on a glass/ITO electrode (electrode I), from a solution containing compound **5a**, 14 wt % of TEGDMA, 7 wt % of TMPTA, and 2 wt % of PMMA in acetonitrile. The films were then subjected to thermal cross linking at 185 °C for 15 h, and a patterned gold electrode (electrode II) was deposited via thermal evaporation.

The counter electrode for electrochromism (electrode III) was prepared by spin coating, onto ITO/glass, a thin layer of a minimally color-changing polymer (MCCP) along with 4 wt % of $TBAPF_6$ from a chloroform solution. MCCP, an *N*-alkyl substituted poly(3,4-propylenedioxypyrrole) derivative similar to that previously reported by our group,[76] was employed as the charge-balancing material. Finally, a gel electrolyte, containing PMMA and $TBAPF_6$ in propylene carbonate, was sandwiched between the ITO/poly-**5a**/gold and ITO/MCCP electrodes.

In this device construction, ITO-coated glass with the active polymer layer was designed to function as both the anode for light emission and the working electrode for electrochromism. As a result, the dual EC/EL prototype allowed for light emission upon the application of bias between the ITO I anode and gold cathode, while the electrochromic mode could be triggered as a result of applying voltage between the electrodes I and III.

Absorption and emission spectra for the device operated in the reflective electrochromic and emissive modes along with the corresponding photographs are given in Figure 7. Respective colorimetric data are summarized in Table S1 in

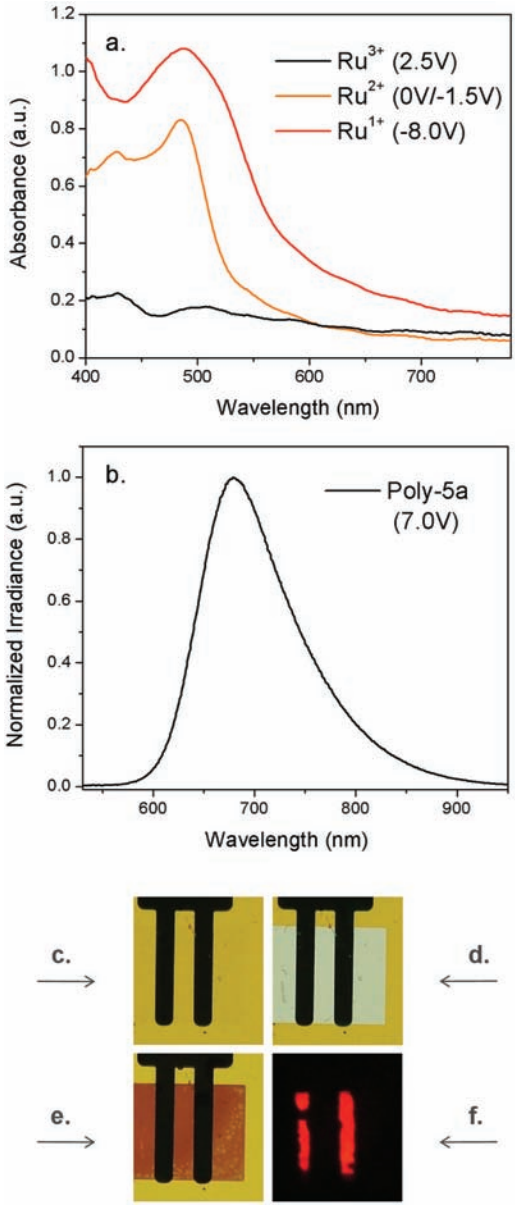

Figure 7. Absorption spectra (a) of a dual EC/EL device pixel as it is operated in the electrochromic mode in the 'as prepared' (Ru^{2+}), oxidized (Ru^{3+}), and reduced (Ru^{1+}) states at the indicated voltages along with the corresponding photographs of the pixel in these states: (c), (d), and (e), respectively. Emission spectra (b) of the device pixel operated in the electrochemiluminescent mode at 7 V along with the corresponding photograph (f).

Supporting Information. As can be seen (Figures 7a,c–e, Table S1, Supporting Information), the electrochromic behavior of the dual EC/EL prototype was, in principle, analogous to that of the poly-**5a** film described previously (Figure 2a, Table 1) with minimal deviations in the absorption spectra and $L^*a^*b^*$ coordinates being caused by the additional MCCP and gel electrolyte layers. As prepared, the device exhibited an orange color (L^*, a^*, b^* = 82, 14, 53), that was switched to a dark red-orange hue (L^*, a^*, b^* = 63, 29, 43) upon reduction at −8 V and reached a nearly colorless highly transmissive state (L^*, a^*, b^* = 90, 5, 5) upon oxidation at 2.5 V. Additionally, the dual EC/EL prototype maintained relatively high $\Delta\%T$ and ΔE values of 53 and 59 (2+ → 3+) as well as 49 and 52 (1+ → 3+),

dx.doi.org/10.1021/ja2065297 | J. Am. Chem.Soc. 2012, 134, 968–978

respectively (Table S1, Supporting Information). It is notable that the color changes occurred across the entire pixel including the area under the gold digits. While prolonged operation under reduced conditions led to device degradation, the prototype could be reversibly switched between the 'as prepared' and oxidized states. Furthermore, this reversibility was preserved as the device was cycled between the EC (oxidation transition) and ECL modes. When operated in the emissive state, as seen in Figure 7, the dual EC/EL prototype exhibited red luminescence with λ_{max} = 680 nm, identical to that previously observed for **5a** solutions, films, and LEC devices (Figures 4, 5, and S5 in the Supporting Information). As this device is unoptimized with rather large pixels, the operating voltage is slightly higher than the individual operations of EC and ECL demonstrated previously. This is not unexpected as there is a fairly significant IR drop across the larger transparent electrode area utilized in this dual device demonstration. Additionally, this prototype performance is highly affected by the nature of the employed gel electrolyte and charge-balancing materials. As a result, it is anticipated that lower operating voltage, brighter light output, and improved evenness in EC and ECL can be obtained with further efforts toward device optimization through engineering. Regardless, this is the first reported demonstration of bright light emission and full EC switching in a single active material when employed as a single layer in a dual EC/EL device.

3. CONCLUSIONS

In conclusion, demonstrated herein is a new series of ruthenium(II) tris(bipyridine)-based coordination complexes that form insoluble films with dual electrochromic/electrochemiluminescent character upon cross-linking. A wide palette of colors is obtained upon electrochemical switching of the polymeric networks. In addition, orange-red to deep red electrogenerated chemiluminescence with λ_{max} ranging from 680 to 722 nm is observed as the Ru(II) polypyridyl complexes are applied in light-emitting electrochemical cell devices. Finally, an EC/EL device prototype is demonstrated where the dual response is achieved from a single Ru(II) complex active layer in a single architecture. This concept has been difficult to achieve in the past as the requirements for a material to exhibit both EC and ECL in the same device are rather stringent. However, due to their reversible redox switching, electroluminescent, and polyelectrochromic behavior as well as the reactive nature of the pendant acrylate moieties cross-linkable ruthenium complexes presented in this study are attractive candidates for well-defined dual EC/EL active layers.

■ ASSOCIATED CONTENT

Ⓢ Supporting Information

Experimental procedures as well as additional synthesis, electrochemical, spectroelectrochemical, photophysical, and device characterization data. This material is available free of charge via the Internet at http://pubs.acs.org.

■ AUTHOR INFORMATION

Corresponding Author

reynolds@chem.ufl.edu

■ ACKNOWLEDGMENTS

The authors would like to thank Emily J. Thompson for her valuable input in the area of colorimetry. Matthew D. Nelson, Caroline M. Grand, Suhas Rao, and Joe Shalosky (University of Florida Machine Shop) are thanked for their contribution to various stages of the dual EC/EL device prototype fabrication and characterization. Funding from Nanoholdings for the initial phase of this effort is gratefully acknowledged. Part of this material (i.e., electrochemical and photophysical data) is based upon work supported as part of the UNC EFRC: Solar Fuels and Next Generation Photovoltaics, an Energy Frontier Research Center funded by the U.S. Department of Energy, Office of Science, Office of Basic Energy Sciences under award number DE-SC0001011.

■ REFERENCES

(1) Forrest, S. R.; Thompson, M. E. *Chem. Rev.* **2007**, *107*, 923−925.
(2) Chen, S.; Deng, L.; Xie, J.; Peng, L.; Xie, L.; Fan, Q.; Huang, W. *Adv. Mater.* **2010**, *22*, 5227−5239.
(3) Monk, P. M. S.; Mortimer, R. J.; Rosseinsky, D. R. *Electrochromism and Electrochromic Devices*; Cambridge University Press: Cambridge, U.K., 2007.
(4) Sekitani, T.; Nakajima, H.; Maeda, H.; Fukushima, T.; Aida, T.; Hata, K.; Someya, T. *Nat. Mater.* **2009**, *8*, 494−499.
(5) Lamansky, S.; Djurovich, P.; Murphy, D.; Abdel-Razzaq, F.; Lee, H.-E.; Adachi, C.; Burrows, P. E.; Forrest, S. R.; Thompson, M. E. *J. Am. Chem. Soc.* **2001**, *123*, 4304−4312.
(6) Kim, S.; Kwon, H.-J.; Lee, S.; Shim, H.; Chun, Y.; Choi, W.; Kwack, J.; Han, D.; Song, M.; Kim, S.; Mohammadi, S.; Kee, I.; Lee, S. Y. *Adv. Mater.* **2011**, *23*, 3511−3516.
(7) Rosseinsky, D. R.; Mortimer, R. J. *Adv. Mater.* **2001**, *13*, 783−793.
(8) Andersson, P.; Forchheimer, R.; Tehrani, P.; Berggren, M. *Adv. Funct. Mater.* **2007**, *17*, 3074−3082.
(9) Sonmez, G.; Meng, H.; Wudl, F. *Chem. Mater.* **2004**, *16*, 574−580.
(10) Reynolds, J. R. Dual Light Emitting and Electrochromic Device. WO 2006045043, April 27, 2006.
(11) Sun, Q.; Li, Y.; Pei, Q. *J. Disp. Technol.* **2007**, *3*, 211−224.
(12) Slinker, J.; Bernards, D.; Houston, P. L.; Abruna, H. D.; Bernhard, S.; Malliaras, G. G. *Chem. Commun.* **2003**, 2392−2399.
(13) Pei, Q.; Yu, G.; Zhang, C.; Yang, Y.; Heeger, A. J. *Science* **1995**, *269*, 1086−1088.
(14) Wang, X. J.; Lau, W. M.; Wong, K. Y. *Appl. Phys. Lett.* **2005**, *87*, 113502/1−113502/3.
(15) Enomoto, S.; Uchikoga, S.; Amanomiya, I.; Nakai, Y. Display Device Using Electrochemiluminescent (ECL) and Electrochromic (EC) Substances. JP 2005128062, May 19, 2005.
(16) Enomoto, S.; Mizuno, Y.; Saito, N. Electrochromic Layer-Involving High-Contrast Organic Electroluminescent Display. JP 2007286561, November 1, 2007.
(17) Watanabe, Y.; Nakamura, K.; Kobayashi, N. *Chem. Lett.* **2010**, *39*, 1309−1311.
(18) Reynolds, J. R.; Dyer, A. L. Interdigitated Electrode Dual Electrochromic/Electroluminescent Devices. WO 2009129275, October 22, 2009.
(19) Juris, A.; Balzani, V.; Barigelletti, F.; Campagna, S.; Belser, P.; Von Zelewsky, A. *Coord. Chem. Rev.* **1988**, *84*, 85−277.
(20) Campagna, S.; Puntoriero, F.; Nastasi, F.; Bergamini, G.; Balzani, V. *Top. Curr. Chem.* **2007**, *280*, 117−214.
(21) Hager, G. D.; Crosby, G. A. *J. Am. Chem. Soc.* **1975**, *97*, 7031−7037.
(22) Tokel, N. E.; Bard, A. J. *J. Am. Chem. Soc.* **1972**, *94*, 2862−2863.
(23) Wallace, W. L.; Bard, A. J. *J. Phys. Chem.* **1979**, *83*, 1350−1357.
(24) Bernhard, S.; Barron, J. A.; Houston, P. L.; Abruna, H. D.; Ruglovksy, J. L.; Gao, X.; Malliaras, G. G. *J. Am. Chem. Soc.* **2002**, *124*, 13624−13628.
(25) Slinker, J. D.; Rivnay, J.; Moskowitz, J. S.; Parker, J. B.; Bernhard, S.; Abruna, H. D.; Malliaras, G. G. *J. Mater. Chem.* **2007**, *17*, 2976−2988.

(26) Elliott, C. M.; Pichot, F.; Bloom, C. J.; Rider, L. S. *J. Am. Chem. Soc.* **1998**, *120*, 6781−6784.
(27) Handy, E. S.; Pal, A. J.; Rubner, M. F. *J. Am. Chem. Soc.* **1999**, *121*, 3525−3528.
(28) Pichot, F.; Beck, J. H.; Elliott, C. M. *J. Phys. Chem. A* **1999**, *103*, 6263−6267.
(29) Elliott, C. M. *J. Chem. Soc., Chem. Commun.* **1980**, 261−262.
(30) Elliott, C. M.; Hershenhart, E. J. *J. Am. Chem. Soc.* **1982**, *104*, 7519−7526.
(31) Elliott, C. M.; Redepenning, J. G. *J. Electroanal. Chem. Interfacial Electrochem.* **1986**, *197*, 219−232.
(32) Elliott, C. M.; Schmittle, S. J.; Redepenning, J. G.; Balk, E. M. *J. Macromol. Sci., Chem.* **1988**, *A25*, 1215−25.
(33) Leasure, R. M.; Ou, W.; Moss, J. A.; Linton, R. W.; Meyer, T. J. *Chem. Mater.* **1996**, *8*, 264−273.
(34) Zhang, H. T.; Subramanian, P.; Fussa-Rydel, O.; Bebel, J. C.; Hupp, J. T. *Sol. Energy Mater. Sol. Cells* **1992**, *25*, 315−325.
(35) Qi, Y.; Desjardins, P.; Wang, Z. Y. *J. Opt. A: Pure Appl. Opt.* **2002**, *4*, S273−S277.
(36) Qi, Y.; Wang, Z. Y. *Macromolecules* **2003**, *36*, 3146−3151.
(37) Ford, P. C.; Wink, D.; Dibenedetto, J. *Prog. Inorg. Chem.* **1983**, *30*, 213−271.
(38) Wacholtz, W. F.; Auerbach, R. A.; Schmehl, R. H. *Inorg. Chem.* **1986**, *25*, 227−234.
(39) Wang, S.; Li, X.; Xun, S.; Wan, X.; Wang, Z. Y. *Macromolecules* **2006**, *39*, 7502−7507.
(40) Santos, L. F.; Gaffo, L.; Magno, d. C. L.; Goncalves, D.; Faria, R. M. *Mol. Cryst. Liq. Cryst. Sci. Technol., Sect. A* **2002**, *374*, 469−474.
(41) Braun, D.; Heeger, A. J. *Appl. Phys. Lett.* **1991**, *58*, 1982−1984.
(42) Wang, H.-M.; Hsiao, S.-H.; Liou, G.-S.; Sun, C.-H. *J. Polym. Sci., Part A: Polym. Chem.* **2010**, *48*, 4775−4789.
(43) Embert, F.; Lere-Porte, J.-P.; Moreau, J. J. E.; Serein-Spirau, F.; Righi, A.; Sauvajol, J.-L. *J. Mater. Chem.* **2001**, *11*, 718−722.
(44) Koyuncu, S.; Usluer, O.; Can, M.; Demic, S.; Icli, S.; Serdar Sariciftci, N. *J. Mater. Chem.* **2011**, *21*, 2684−2693.
(45) Koldemir, U.; Graham, K. R.; Salazar, D. H.; McCarley, T. D.; Reynolds, J. R. *J. Mater. Chem.* **2011**, *21*, 6480−6482.
(46) Cao, Y.; Pei, Q.; Andersson, M. R.; Yu, G.; Heeger, A. J. *J. Electrochem. Soc.* **1997**, *144*, 317−320.
(47) Grabulosa, A.; Beley, M.; Gros, P. C. *Eur. J. Inorg. Chem.* **2008**, 1747−1751.
(48) Anderson, T. J.; Scott, J. R.; Millett, F.; Durham, B. *Inorg. Chem.* **2006**, *45*, 3843−3845.
(49) Wang, Z. Y. Ruthenium Complexes for Organic Electrochromic Materials for Optical Attenuation in the Near Infrared Region. US 20030066989, April 10, 2003.
(50) Yu, S. C.; Hou, S.; Chan, W. K. *Macromolecules* **2000**, *33*, 3259−3273.
(51) Calvert, J. M.; Schmehl, R. H.; Sullivan, B. P.; Facci, J. S.; Meyer, T. J.; Murray, R. W. *Inorg. Chem.* **1983**, *22*, 2151−2162.
(52) Schanda, J. D. In *Handbook of Applied Photometry*; DeCusatis, D. C., Ed.; Optical Society of America: New York, 1998.
(53) *CIE Publication no. 15.2, Colorimetry*; National Physical Laboratory: Middlesex, U.K., 1986.
(54) Thompson, B. C.; Schottland, P.; Zong, K.; Reynolds, J. R. *Chem. Mater.* **2000**, *12*, 1563−1571.
(55) Amb, C. M.; Dyer, A. L.; Reynolds, J. R. *Chem. Mater.* **2011**, *23*, 397−415.
(56) Ohta, N.; Robertson, A. R. *Colorimetry: Fundamentals and Applications*; Jonn Wiley & Sons Ltd.: Chichester, U.K., 2005.
(57) Dyer, A. L.; Craig, M. R.; Babiarz, J. E.; Kiyak, K.; Reynolds, J. R. *Macromolecules* **2010**, *43*, 4460−4467.
(58) Amb, C. M.; Kerszulis, J. A.; Thompson, E. J.; Dyer, A. L.; Reynolds, J. R. *Polym. Chem.* **2011**, *2*, 812−814.
(59) Dyer, A. L.; Thompson, E. J.; Reynolds, J. R. *ACS Appl. Mater. Interfaces* **2011**, *3*, 1787−1795.
(60) Forster, L. S. *Coord. Chem. Rev.* **2006**, *250*, 2023−2033.
(61) Lytle, F. E.; Hercules, D. M. *J. Am. Chem. Soc.* **1969**, *91*, 253−257.
(62) Yang, X. J.; Janiak, C.; Heinze, J.; Drepper, F.; Mayer, P.; Piotrowski, H.; Klufers, P. *Inorg. Chim. Acta* **2001**, *318*, 103−116.
(63) Caspar, J. V.; Meyer, T. J. *J. Phys. Chem.* **1983**, *87*, 952−957.
(64) Caspar, J. V.; Kober, E. M.; Sullivan, B. P.; Meyer, T. J. *J. Am. Chem. Soc.* **1982**, *104*, 630−632.
(65) Barigelletti, F.; Juris, A.; Balzani, V.; Belser, P.; Von Zelewsky, A. *Inorg. Chem.* **1983**, *22*, 3335−3339.
(66) Rudmann, H.; Shimada, S.; Rubner, M. F. *J. Appl. Phys.* **2003**, *94*, 115−122.
(67) Buda, M.; Kalyuzhny, G.; Bard, A. J. *J. Am. Chem. Soc.* **2002**, *124*, 6090−6098.
(68) Bolink, H. J.; Cappelli, L.; Coronado, E.; Graetzel, M.; Nazeeruddin, M. K. *J. Am. Chem. Soc.* **2006**, *128*, 46−47.
(69) Soltzberg, L. J.; Slinker, J. D.; Flores-Torres, S.; Bernards, D. A.; Malliaras, G. G.; Abruna, H. D.; Kim, J.-S.; Friend, R. H.; Kaplan, M. D.; Goldberg, V. *J. Am. Chem. Soc.* **2006**, *128*, 7761−7764.
(70) Kalyuzhny, G.; Buda, M.; McNeill, J.; Barbara, P.; Bard, A. J. *J. Am. Chem. Soc.* **2003**, *125*, 6272−6283.
(71) Liu, C.-Y.; Bard, A. J. *J. Am. Chem. Soc.* **2002**, *124*, 4190−4191.
(72) Rudmann, H.; Rubner, M. F. *J. Appl. Phys.* **2001**, *90*, 4338−4345.
(73) He, L.; Qiao, J.; Duan, L.; Dong, G.; Zhang, D.; Wang, L.; Qiu, Y. *Adv. Funct. Mater.* **2009**, *19*, 2950−2960.
(74) Rudmann, H.; Shimada, S.; Rubner, M. F. *J. Am. Chem. Soc.* **2002**, *124*, 4918−4921.
(75) Bolink, H. J.; Coronado, E.; Costa, R. D.; Gavina, P.; Orti, E.; Tatay, S. *Inorg. Chem.* **2009**, *48*, 3907−3909.
(76) Walczak, R. M.; Reynolds, J. R. *Adv. Mater.* **2006**, *18*, 1121−1131.